

Spectral Reflectance Estimation of Human Skin and Its Application to Image Rendering

Motonori Doi[▲]

Department of Telecommunication and Computer Networks, Osaka Electro-Communication University, Neyagawa, Osaka, JAPAN

Norihiro Tanaka

Department of Industry-Information Science, Nagano University, Ueda, Nagano, JAPAN

Shoji Tominaga[▲]

Department of Engineering Informatics, Osaka Electro-Communication University, Neyagawa, Osaka, JAPAN

The analysis and synthesis of human skin color is important in many application areas. The skin color depends on some histological variables such as the concentration of pigments melanin and hemoglobin in skin layers. The present paper proposes a method for estimating the surface spectral reflectance of human skin based on an optics model and applying the estimates to 3D realistic image rendering for a human hand. The human skin is modeled as the two layers of the turbid materials for the epidermis and dermis. An estimation algorithm for the two layer model is then developed using the Kubelka–Munk theory. The parameters representing the concentration of pigments are determined based on spectral reflectance measurements of the human skin surface. In the application step, we describe a technique for rendering realistic skin images of a skin surface as a 3D object. The Torrance–Sparrow model is adapted in the image rendering process. The accuracy of the estimated reflectances is shown in experiments, and skin color images are created under a variety of illumination, viewing, and pigmentation conditions.

Journal of Imaging Science and Technology 49: 574–582 (2005)

Introduction

The analysis and synthesis of human skin color has attracted increased attention in many different application areas, including computer graphics and multimedia,^{1–3} medical imaging and diagnosis,^{4,5} and cosmetic applications.⁶ It is known that the skin color depends primarily on some histological variables such as the concentration of pigments of melanin and hemoglobin in skin layers and the thickness and depth of the layers.⁷ The variables are inherent to individual persons and body parts. These are usually influenced by several conditions, such as the mental condition of the human's emotions, the physical condition of tanning, or the medical condition of inflammation.

The modeling of skin coloration has its origin in the description of the interaction between incident light and pigments in the skin layers. An optical model based on the Lambert–Beer law was used for the estimation of

skin color.^{1,2,6} The Lambert–Beer law is useful for describing the light transmission property. However, this law takes account of only the light absorption by pigments in a medium, whereas human skin color is caused mainly by strong back scattering of light within the skin layers. Another reason why the Lambert–Beer law is not exactly applicable is that the transmittance is not measured *in vivo*, but only the reflectance measurements of the skin surface are available for analyzing skin color.

The Monte Carlo technique is known as a flexible method for simulating the propagation of light in skin tissues.^{4,5} The simulation is based on the random walks that photons make as they travel through the tissue, which are chosen by statistically sampling a probability distribution on scattering. Although this technique can be used to simulate the skin coloration model and estimate the surface reflectance, it is not easy to determine the probability of the photons random moves from the reflectance measurements.

Kubelka and Munk formulated the optical radiation transfer involving absorption and scattering in a turbid medium.^{8,9} The Kubelka–Munk theory offers a useful means for quantitative treatment of skin optics because the two skin layers of epidermis and dermis are assumed to consist of inhomogeneous and turbid materials. The absorption and scattering coefficients can be determined

Original manuscript received July 13, 2004

▲ IS&T Member

Corresponding Author: M. Doi, Doi@isc.osakac.ac.jp

©2005, IS&T—The Society for Imaging Science and Technology

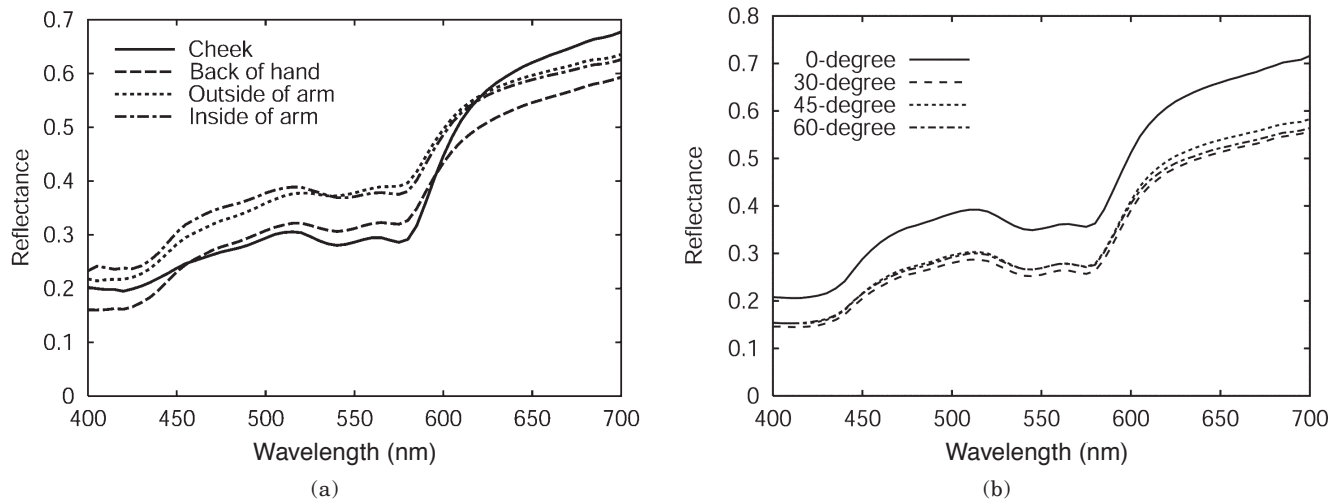


Figure 1. Surface spectral reflectances of real skin. (a) Measurements at different skin surfaces of the human body. (b) Measurements with different lighting directions at a skin surface.

from reflectance measurements of the material.⁸ There are previous works on skin optics using the Kubelka–Munk theory.^{10–13} Anderson et al.,^{10,11} discussed the transfer of optical radiation into human skin, aimed at developing models for photomedicine. Van Gemert et al.¹² discussed skin tissue optics in the context of the treatment of skin disorders and collected optical data on human skin. The data published in these papers are valuable and used in this paper. Cotton et al.¹³ proposed a mathematical model of color formation. Although the dermis was modeled with the Kubelka–Munk theory, the epidermis was approximated with Bouguer’s law (Lambert–Beer law).¹⁴ This work did not estimate surface spectral reflectance of human skin. Moreover, when comparing scattering coefficients between epidermis and dermis, we cannot neglect the scattering effect in the epidermis or in the dermis.¹² The Kubelka–Munk theory should be adopted to both layers of the epidermis and dermis.

In this article we describe a method for estimating the surface spectral reflectance of human skin based on a skin optics model. The application of these estimates to three-dimensional (3D) image rendering of a human body part is also described. In the first step of the reflectance estimation, the human skin is modeled as two layers of turbid materials, one for the epidermis and the other one for the dermis. An estimation algorithm is developed using the Kubelka–Munk theory applied to the two layer model. The parameters representing the concentration of pigments are determined based on spectral reflectance measurements of the human skin surface using a calibrated system of a spectrometer, a light source, and a standard white target.

In the application step, a technique for rendering realistic skin images of the human body as a 3D object is described. We assume that light reflected from skin is decomposed into two components: the diffuse reflection component based on absorption and scattering in the skin layers and the specular reflection component occurring at the interface between the outer skin layer and air. We assume the diffuse reflection to be Lambertian. Moreover, we assume the specular reflection to occur at micro facets. Hence, we describe the diffuse component by the Lambertian model and the specular component by the Torrance–Sparrow model. The entire

3D reflection model combining the two models is called the Torrance–Sparrow model for simplicity throughout this paper. In the experiments, skin color images are created under a variety of illumination, viewing, and pigmentation conditions.

Some essential points of the proposed method are listed as follows:

1. The proposed method does not estimate a RGB color model for describing human skin because of its device dependence, but it does estimate a surface spectral reflectance function that is inherent in human skin.
2. The skin layers are represented as a two layer model of turbid materials for the epidermis and dermis; the surface spectral reflectance is estimated using the Kubelka–Munk theory.
3. Realistic color images for a part of the human body are created under a variety of conditions by using the 3D reflection model with the estimated surface reflectance and the rendering algorithm.

Skin Optics Model

The surface spectral reflectance observed from a skin surface is described with the dichromatic reflection model

$$R(\lambda) = R_b(\lambda) + R_s(\lambda) \quad (1)$$

where $R_b(\lambda)$ is the diffuse reflection component from inside of the skin and the $R_s(\lambda)$ is the specular reflection component occurring at the interface of skin and air. The specular reflection is observed within a limited range of the viewing angle, and the diffuse reflection is independent of the viewing angle. Figure 1 shows examples of surface spectral reflectance functions of real skin, which were measured under different conditions by using a tungsten halogen lamp, a spectroradiometer, and a white standard plate. Figure 1(a) shows the spectral reflectance curves at different skin surfaces of a human body, where the sensor was placed in the direction of the surface normal and the skin surfaces were illuminated at an angle of 45° relative to the surface normal. Figure 1(b) shows the spectral reflectances measured from the back of a hand with different illumination angles. The spectral curve for normal incidence

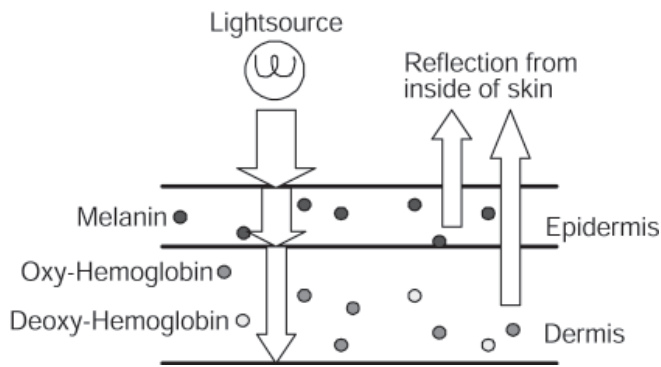


Figure 2. Skin optics model.

(0°) separated from the others includes the specular reflection component.

We analyze the spectral reflectance curves without the specular component in the visible wavelength range of 400–700 nm. A basic feature of the reflectance curves is that the reflectances increase almost monotonically as the wavelength increases. A special feature is the “W” shaped or “U” shaped hollow in the range from 520 nm to 600 nm. This change in reflectance is caused by the absorption of hemoglobin. The spectral reflectance curve of skin is influenced by the interaction of pigments inside the skin tissue.

Figure 2 shows an optics model representing the relationship between light and pigments in the two skin layers. The incident light penetrating the skin surface is absorbed and scattered in the two layers. It should be noted that the optical interactions of scattering, refraction, and absorption in each layer of tissue depends on the wavelength. The two layer model consists of epidermis and dermis. The epidermis includes the melanin pigments. The dermis includes the pigments of oxyhemoglobin, deoxyhemoglobin, and bilirubin. Because of the small amount of bilirubin in healthy skin, the main pigments for skin coloration are the melanin, oxyhemoglobin and deoxyhemoglobin. A hypodermis is under the dermis. This material is white fat. Therefore, surface reflectance for the hypodermis layer can be assumed to have a constant spectral response of unity. The possibility of light reaching the hypodermis is, in any case, quite low.

The Kubelka–Munk Theory

In general, the Kubelka–Munk theory^{8,9} is convenient for calculating the optical values of reflectance and transmittance within a layer consisting of turbid materials. We assume that the skin optics model of Fig. 2 has two layers of turbid materials. Figure 3 shows a model of the Kubelka–Munk equations for radiation transfer in a single layer of turbid material (also see Ref. 11). The symbol I is defined as the intensity of light traveling inside a plane parallel light scattering medium towards its unilluminated surface, and the symbol J is defined as the intensity of light traveling in the reverse direction. Moreover, I_0 is the intensity of the incident light, J_0 is the intensity of reflected light from the illuminated surface, and I_D is the intensity of the transmitted light from the unilluminated surface. The symbol x is the distance from the illuminated surface, that is the depth measured from the surface at $x = 0$, and D is the thickness of the layer.

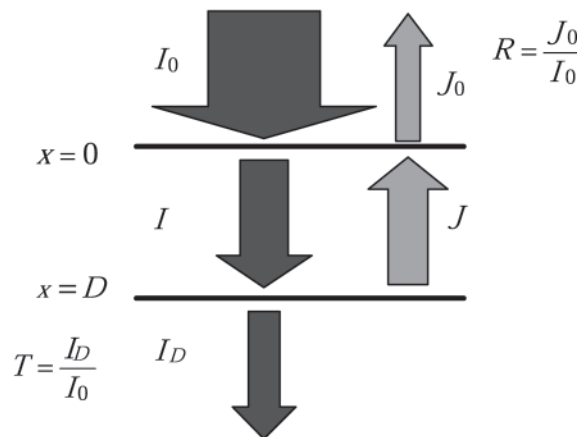


Figure 3. Model for the Kubelka–Munk equations for a single layer.

The relationship between the light intensities I and J is described as a system of two differential equations in the variable of depth, x :

$$\begin{aligned} \frac{dI}{dx} &= -SI - KI + SJ \\ -\frac{dJ}{dx} &= -SJ - KJ + SI \end{aligned} \quad (2)$$

where S and K are, respectively, the coefficients of back-scattering and absorption in the media.

The reflectance R and the transmittance T of the turbid layer with a thickness D is derived by solving the above equations with some mathematical approximations as follows:

$$\begin{aligned} R = J_0 / I_0 &= \frac{1}{a + b \coth(bSD)} \\ T = I_D / I_0 &= \frac{b}{a \sinh(bSD) + b \coth(bSD)} \end{aligned} \quad (3)$$

where

$$a \equiv \frac{S+K}{S}, \quad b \equiv \sqrt{a^2 - 1}$$

Because of the two layer model, we have to consider multiple reflections at the interface between the higher layer (Layer 1) of epidermis and the lower layer (Layer 2) of dermis as shown in Fig. 4 (see Ref. 9). The total reflectance $R_{1,2}$ for the two layers including the inter-reflection is described as

$$\begin{aligned} R_{1,2} &= R_1 + T_1^2 R_2 (1 + R_1 R_2 + \dots) \\ &= R_1 + \frac{T_1^2 R_2}{1 - R_1 R_2} \end{aligned} \quad (4)$$

where T_1 and R_1 are, respectively, the transmittance and reflectance of Layer 1, and R_2 is the reflectance on Layer 2. In the skin model, the base layer of hypodermis is beneath Layer 2 of dermis. Therefore, R_2 includes the reflection from the hypodermis layer.

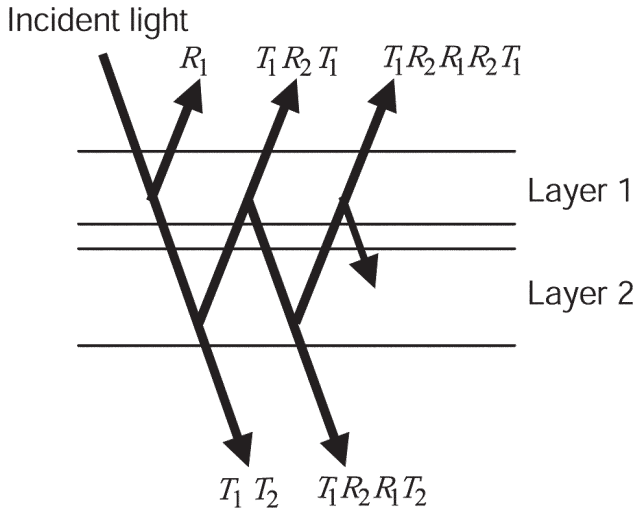


Figure 4. Different paths of the diffused light for the two layered model.

Estimation Algorithms of Surface-spectral Reflectance

The solution of the Kubelka–Munk equations is applied to the skin optics model for estimating the surface spectral reflectance function of human skin. The body reflectance function $R_b(\lambda)$ of the skin surface is described as a function of wavelength as

$$R_b(\lambda) = R_e(\lambda) + \frac{T_e(\lambda)^2 R_{dt}(\lambda)}{1 - R_e(\lambda)R_{dt}(\lambda)}, \quad (5)$$

where $R_e(\lambda)$ and $T_e(\lambda)$ are, respectively, the spectral reflectance and transmittance of epidermis. The spectral reflectance $R_{dt}(\lambda)$ represents the reflectance of dermis upon a backing from which the transmitted light is reflected back to the dermis by the white surface of the hypodermis with reflectance $R = 1$. We thus immediately get an equation for $R_{dt}(\lambda)$ as

$$R_{dt}(\lambda) = R_d(\lambda) + \frac{T_d(\lambda)^2}{1 - R_d(\lambda)}, \quad (6)$$

where $R_d(\lambda)$ and $T_d(\lambda)$ are the spectral reflectance and transmittance of the dermis, respectively.

The spectral reflectances and transmittances of the respective layers are given as follows:

Epidermis:

$$\begin{aligned} R_e(\lambda) &= \frac{1}{a_e(\lambda) + b_e(\lambda) \coth(C_e(\lambda))} \\ T_e(\lambda) &= \frac{b_e(\lambda)}{a_e(\lambda) \sinh(C_e(\lambda)) + b_e(\lambda) \coth(C_e(\lambda))} \\ a_e(\lambda) &= \frac{S_e(\lambda) + K_{et}(\lambda)}{S_e(\lambda)} \\ b_e(\lambda) &= \sqrt{a_e(\lambda)^2 - 1} \\ C_e(\lambda) &\equiv D_e b_e(\lambda) S_e(\lambda) \end{aligned} \quad (7)$$

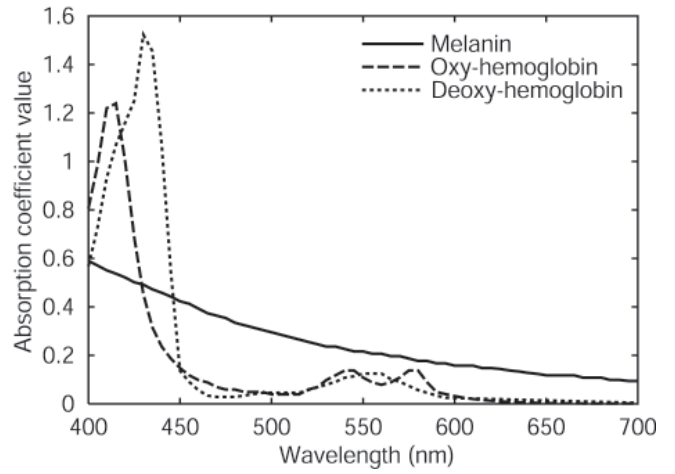


Figure 5. Spectral absorption coefficients of pigments (after Ref. 10).

Dermis:

$$\begin{aligned} R_d(\lambda) &= \frac{1}{a_d(\lambda) + b_d(\lambda) \coth(C_d(\lambda))} \\ T_d(\lambda) &= \frac{b_d(\lambda)}{a_d(\lambda) \sinh(C_d(\lambda)) + b_d(\lambda) \coth(C_d(\lambda))} \\ a_d(\lambda) &= \frac{S_d(\lambda) + K_{dt}(\lambda)}{S_d(\lambda)} \\ b_d(\lambda) &= \sqrt{a_d(\lambda)^2 - 1} \\ C_d(\lambda) &\equiv D_d b_d(\lambda) S_d(\lambda) \end{aligned} \quad (8)$$

The spectral scattering coefficients $S_e(\lambda)$ and $S_d(\lambda)$ in epidermis and dermis are determined mostly by the media, because scattering caused by the pigments is relatively small; e.g., see Ref. 12. On the other hand, the spectral absorption coefficients $K_{et}(\lambda)$ and $K_{dt}(\lambda)$ in the two layers are determined by the pigments in the following forms:

$$\begin{aligned} K_{et}(\lambda) &= w_m K_m(\lambda) \\ K_{dt}(\lambda) &= w_h K_h(\lambda) + w_{dh} K_{dh}(\lambda) \end{aligned} \quad (9)$$

where $K_m(\lambda)$, $K_h(\lambda)$, and $K_{dh}(\lambda)$ represent the spectral absorption coefficients of melanin, oxyhemoglobin, and deoxyhemoglobin, respectively. The constant coefficients w_m , w_h , and w_{dh} represent the weights of the pigment absorption coefficients.

Thus, the problem of estimating the surface spectral reflectance function of human skin can be reduced to the determination of the weighting coefficients for three pigments when $S_e(\lambda)$, $S_d(\lambda)$, $K_m(\lambda)$, $K_h(\lambda)$, and $K_{dh}(\lambda)$ are known. For applying the estimation algorithm to real measurements, we need the optical and histological data of skin tissue. We have referred to previous works for information about such reference data. The spectral absorption data, the spectral scattering data, and the layer thickness values published in Refs. 10 through 12 are used in this article. Figure 5 shows the spectral curves of the absorption coefficients $K_m(\lambda)$, $K_h(\lambda)$, and $K_{dh}(\lambda)$ for three pigments. Figure 6 shows the spectral curves of the scattering coefficients $S_e(\lambda)$ and $S_d(\lambda)$. We

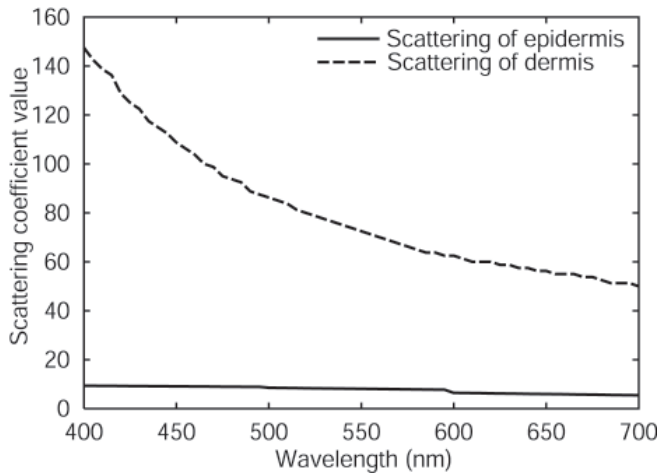


Figure 6. Spectral scattering coefficients of skin (after Refs. 11 and 12).

neglect the light absorption by the medium without pigments in the epidermis and the dermis. The thickness of the epidermis and dermis, D_e and D_d , depend on body parts. We use the anatomical data for these values.¹⁴

Color Image Rendering of Human Skin

Computer graphics images are created using the estimates obtained for the surface spectral reflectance of human skin. We use a ray tracing technique for rendering a computer graphics scene of 3D human bodies, where the visible surfaces in a scene are mapped to a screen image by ray tracing.

Several mathematical models were proposed for describing light reflection of 3D objects, such as the Phong model,¹⁵ the Torrance–Sparrow model,¹⁶ and the Cook–Torrance model.¹⁷ The Phong model is a simple model for 3D computer graphics. The Torrance–Sparrow model is a physically based model. The Cook–Torrance model is a modified version of the Torrance–Sparrow model of the specular functions. In our earlier study, we suggested that the original Torrance–Sparrow model based on direct measurements of some dielectric materials by using a goniospectrometer is an appropriate model.¹⁸ The present paper, too, uses the Torrance–Sparrow model for rendering 3D images of human skin.

The spectral distribution of radiance $Y(\lambda)$ from a skin surface microfacet is described as

$$Y(\lambda) = \alpha(\mathbf{N} \cdot \mathbf{L})R_b(\lambda)E(\lambda) + \beta \frac{DF}{\mathbf{N} \cdot \mathbf{V}}E(\lambda) \quad (10)$$

where the first and second terms represent the diffuse and specular reflection components respectively. Parameters α and β are weighting coefficients. Three vectors \mathbf{N} , \mathbf{L} , and \mathbf{V} represent the normal vector of the surface, the incident light vector, and the view vector, respectively. $R_b(\lambda)$ is the body spectral reflectance of the human skin surface that is estimated as described in the previous section. $E(\lambda)$ is the spectral distribution of the illumination. D is a function representing the distribution of microfacet orientations, and F is a function representing the Fresnel reflectance. These functional forms are given in references; e.g., see Ref. 19.

The color image of human skin is created by spectral computation on the 3D body parts model as follows. First

TABLE I. Thickness of Skin Layers at Different Parts of the Human Body in a Unit mm.¹⁴

| | Cheek | Back of hand | Outside of arm | Inside of arm |
|----------------------|-------|--------------|----------------|---------------|
| Epidermis D_e (mm) | 0.027 | 0.035 | 0.036 | 0.041 |
| Dermis D_d (mm) | 1.491 | 1.190 | 1.403 | 1.294 |

the spectral power distribution of light reflected from the skin surfaces is computed over the visible range, 400 to 700 nm. All spectra are sampled at 5 nm intervals, resulting in a description in the form of 61-dimensional vectors. After the spectral radiant computations, the pixels' color is determined in terms of the tristimulus values CIE-XYZ. Finally the image is generated on a calibrated display device.

Because of the three variable parameters w_m , w_h , and w_{dh} in the skin model, we can create a variety of images with different color appearances of human skin by controlling these parameters. For instance, increasing the weight w_m for the melanin absorption can imitate a sunburn skin. Increasing the weight w_h for oxyhemoglobin absorption can imitate a skin with inflammation symptoms.

Experiments

Experiments were conducted for examining the accuracy of the estimated surface spectral reflectance for different parts of the human body and evaluating the achieved degree of realism of the skin color in the rendered images of a human hand under a variety of conditions.

Measurements

The light reflected from human skin surfaces was measured with spectroradiometer under the light source of a halogen lamp. The spectral reflectance was obtained as the radiance factor,²⁰ which is the ratio of the radiance from a given skin surface patch to the radiance from a perfect reflecting diffuser illuminated in the same way as the skin surface. Hence, a standard reference white target was placed on the same portion of the skin surface for calibrating the reflected light. The incident angle of illumination was about 45°. The spectroradiometer, which has a visual field of 1°, was placed at a distance of 1.2 m from the surfaces and was oriented the direction of the surface normal. This measurement setup helps to exclude the specular reflection component from the reflection of the skin surfaces.

The subjects were three young Japanese: subject A was a 32 year old man, subject B was a 22 year old man, and subject C was a 22 year old woman. The reflectance measurement for each subject was carried out on the four body parts of the cheek, back of the hand, outside of the arm, and inside of the arm. Table I shows the thickness data for the skin layers used in this paper, which are taken from the anatomical data by Yazawa.¹⁴

Reflectance Estimation Results

The three weights w_m , w_h , and w_{dh} of the pigment absorption coefficients of melanin, oxyhemoglobin and deoxyhemoglobin were determined such that the estimated spectral reflectance function $R_b(\lambda)$ of Eq. (5) was fitted to the measured spectral reflectances in the sense of the least squared error. Table II shows the estimated weights for Subject A. Figure 7 shows a set of estimation results of the skin spectral reflectances for Subject A. In each graph of Fig. 7, the solid curve, broken

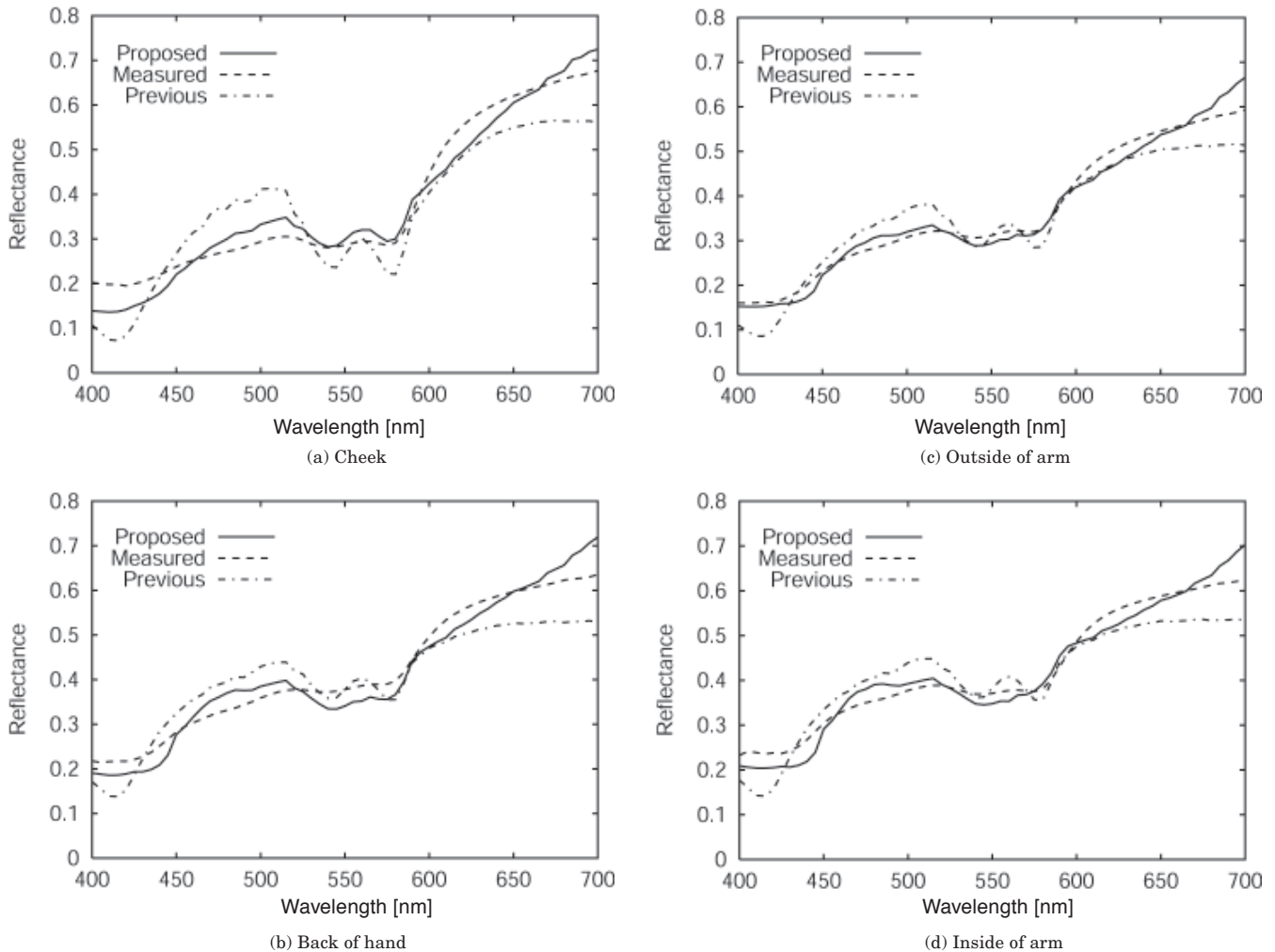


Figure 7. Estimation results of the skin spectral reflectances for Subject A.

curve, and dotted curve represent, respectively, the estimate by the proposed method, the direct measurement, and the estimate by the previous method of Cotton et al.¹³ We recalled that Cotton et al. used Bouguer’s law for the epidermis and used the Kubelka–Munk theory only for dermis. They also took account of light absorption by the dermal tissue. We see in Fig. 7 that good agreement between the estimates and measurements for the back of the hand, the outside of the arm, and the inside of the arm can be obtained using our method. We find a certain discrepancy between the two curves at about 500 nm for the cheek. Moreover, the estimation accuracy is much improved in comparison with the previous method.

Table III summarizes the least squared errors between the estimates and the measurements for all subjects by using the two methods. These comparisons emphasize the accuracy of the proposed estimation method.

Image Rendering Results

Image rendering of a 3D object requires the optical data of the surface reflection and the geometric data of the surface shape. In this study we measured the 3D shape of the human hand by using a laser range finder. We measured the specular reflection component of a human skin for determining the specular function in the Torrance–Sparrow model. First, the skin surface

TABLE II. Pigment Absorption Weights Estimated for Subject A

| | Melanin w_m | Oxyhemoglobin w_n | Deoxyhemoglobin w_{dn} |
|----------------|---------------|---------------------|--------------------------|
| Cheek | 454 | 278 | 50 |
| Back of hand | 384 | 152 | 222 |
| Outside of arm | 276 | 152 | 170 |
| Inside of arm | 234 | 84 | 264 |

reflectances were observed by changing the illumination direction and by fixing the viewing direction to about 60°. Second, a polarizing filter was used for extracting the specular component. Then, the functions in the specular term of Eq. (10) were determined empirically.

Figure 8 shows images of a human hand rendered under the light sources of CIE Standard Illuminants D65 and A, where both illumination and viewing directions are in the normal direction. The estimated spectral reflectance in Fig. 7(b) was used for the diffuse spectral reflectance of skin surface in these images. A visual experiment was carried out by comparing the displayed images on a calibrated CRT monitor to the real hand of the same subject under the two lamps. These comparisons showed good coincidence between the created images and the real object.

TABLE III. Least Squared Errors between the Estimated Reflectances and the Measured Ones

| | | Cheek | Back of hand | Outside of arm | Inside of arm |
|-----------|----------|-------|--------------|----------------|---------------|
| Subject A | Proposed | 0.075 | 0.030 | 0.063 | 0.047 |
| | Previous | 0.352 | 0.117 | 0.204 | 0.161 |
| Subject B | Proposed | 0.031 | 0.015 | 0.016 | 0.021 |
| | Previous | 0.130 | 0.090 | 0.086 | 0.106 |
| Subject C | Proposed | 0.097 | 0.058 | 0.069 | 0.049 |
| | Previous | 0.263 | 0.163 | 0.248 | 0.260 |
| Average | Proposed | 0.068 | 0.034 | 0.049 | 0.039 |
| | Previous | 0.248 | 0.123 | 0.179 | 0.176 |

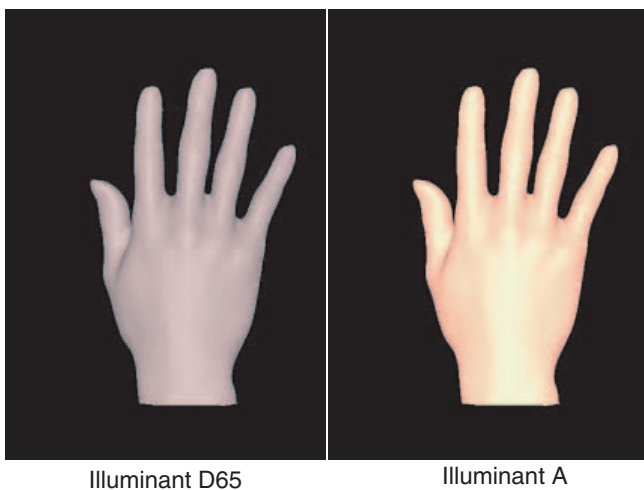
**Figure 8.** Hand images under two illuminants.

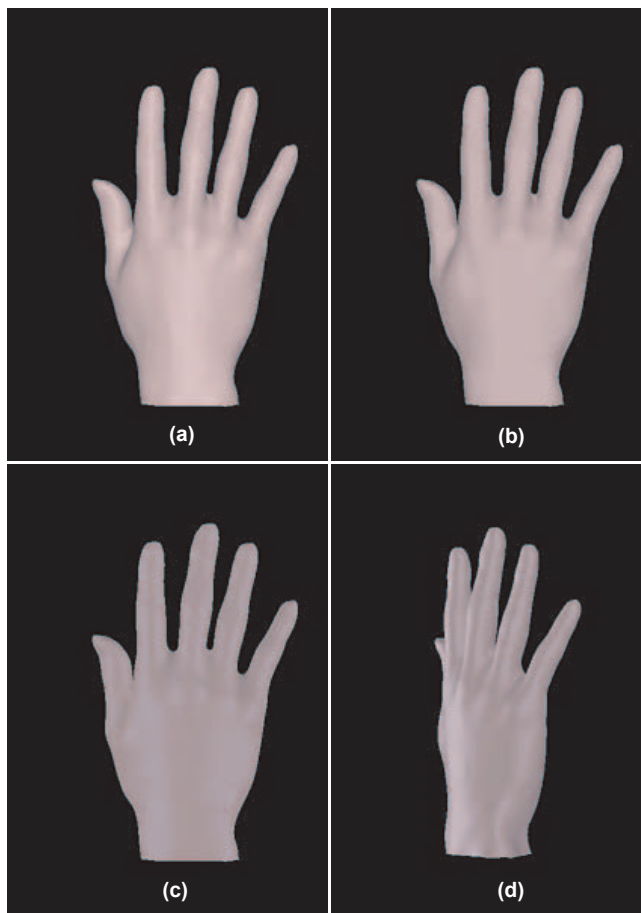
Figure 9 shows different images of the same hand by changing the angles of illumination and viewing. Figure 9(a), 9(b), and 9(c) were created under the illumination angles of 0, 30, and 60°, respectively, and Fig. 9(d) was generated with 60° for both illumination and viewing, that is under the condition of (60/60). Note that a specular reflection component appears on some parts of the skin surface in Fig. 9(d).

Moreover, we created different appearances of the human hand by changing the weighting coefficients of the pigment absorption. Figure 10 shows a set of rendered images, which are arranged on the two scales of the weights for melanin and oxyhemoglobin. The increase of melanin leads to the appearance of sunburn, and the increase of oxyhemoglobin leads to reddish skin. However, note that skin color with a large amount of melanin is not always reddish, as it is not influenced much by hemoglobin. The skin color in the lower layer is supposedly covered with the melanin pigments in the upper layer. These images suggest that a variety of appearance of human skin color can be produced easily by changing the weights of the component pigments.

Thus, the generated computer graphics images represent a realistic appearance of a human hand that is sufficiently close to the real one.

Conclusions

The present paper has described a method for estimating the surface spectral reflectance of human skin based

**Figure 9.** Hand images by changing the angles of illumination and viewing; (a) (0/0); (b) (30/0); (c) (60/0); and (d) (60/60).

on an optics model, and the estimates have been applied to 3D realistic image rendering for a part of a human hand. The human skin was modeled as two layers of turbid materials for epidermis and dermis. An estimation algorithm was then developed by applying the Kubelka–Munk theory to the two layer model. This algorithm includes three unknown parameters representing weights for spectral absorption of such different pigments as melanin, oxyhemoglobin and deoxyhemoglobin. These parameters were determined based on spectral reflectance measurements of human skin surfaces by using a calibrated system of a spectrometer, a light source, and a standard white target.

In the application step, we have described a technique for rendering realistic images of a skin surface as a 3D object. The Torrance–Sparrow model was used as a 3D light reflection model for image rendering. In our experiments, the accuracy of the estimated surface spectral reflectances of human skin was confirmed through a comparison of the estimates and the direct measurements. We have created computer graphics images of a human hand under a variety of conditions. A visual examination of appearances of the rendered objects showed the feasibility of the proposed method.

Real human skin includes surface texture and color variations on its surface.²¹ Our future works is to extend the proposed method to image rendering of skin surface including such complicated structures.

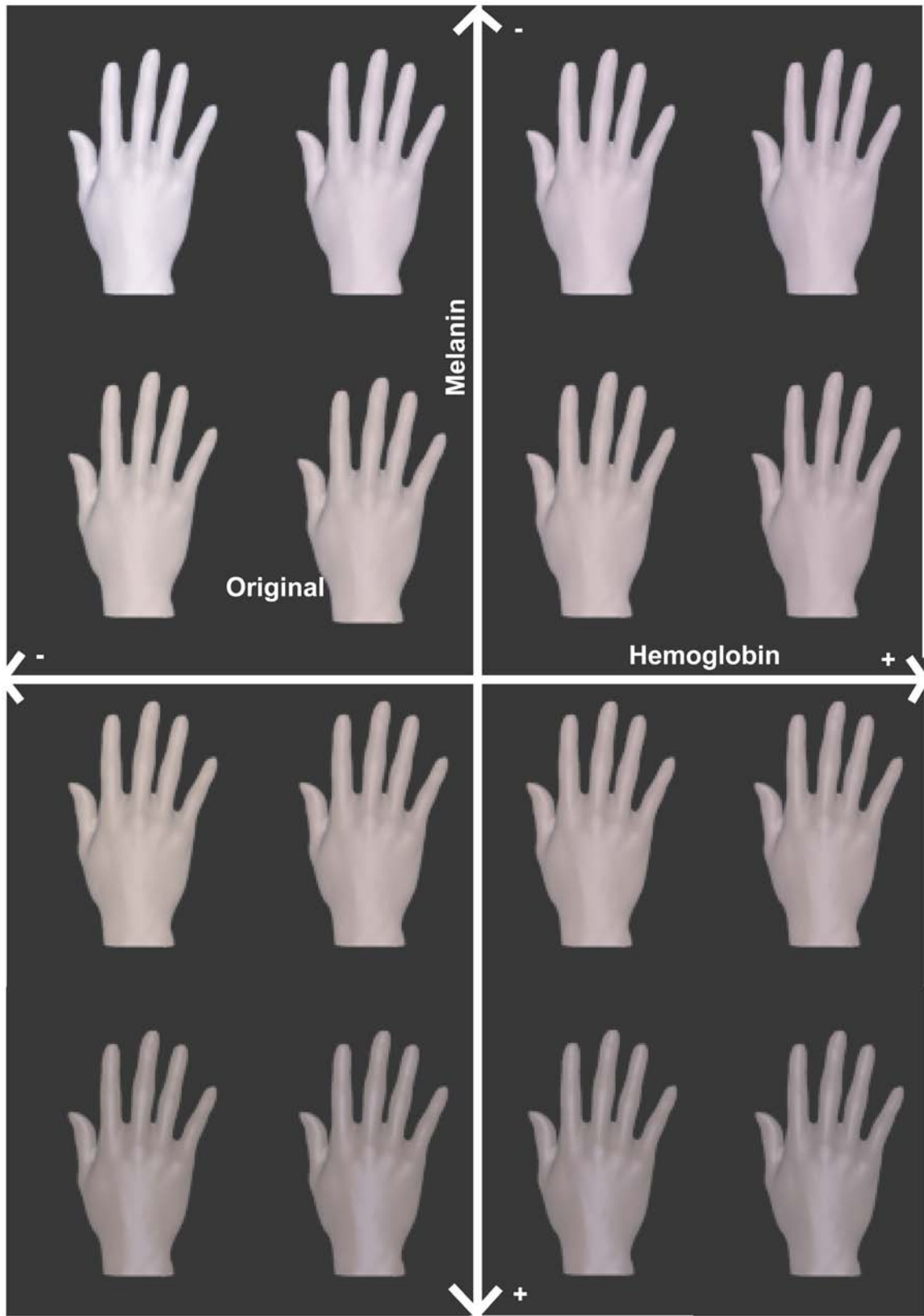


Figure 10. Hand images with the different weights for melanin and hemoglobin

References

1. S. J. Preece and E. Claridge, "Spectral filter optimization for the recovery of parameters which describe human skin", *IEEE Trans. PAMI*, **26**(7), 913 (2004).
2. N. Tsumura, N. Ojima, K. Sato, M. Shiraishi, H. Shimizu, H. Nabeshima, S. Akazaki, K. Hori, and Y. Miyake, "Image-based skin color and texture analysis/synthesis by extracting hemoglobin and melanin information in the skin", *ACM Trans. Graphics*, **22**(3), 770 (2003).
3. E. Angelopoulou, R. Molana and K. Danilidis, "Multispectral skin color modeling", *Proc. IEEE Conf. Computer Vision and Pattern Recognition*, 635 (2001).
4. N. Tsumura, M. Kawabuchi, H. Haneishi, and Y. Miyake, "Mapping pigmentation in human skin from a multi-channel visible spectrum image by inverse optical scattering technique", *J. Imaging Sci. Technol.* **45**(5), 444 (2001).
5. A. Krishnaswamy and G. V. G. Baranoski, "A biophysically-based spectral model of light interaction with human skin", *Computer Graphics Forum*, **23**(4), 331 (2004).
6. N. Ojima, S. Akazaki, K. Hori, N. Tsumura, and Y. Miyake, "Application of image-based skin chromophore analysis to cosmetics", *J. Imaging Sci. Technol.* **48**(3), 222 (2004).
7. H. Takiwaki, Y. Kanno, Y. Miyaoka, and S. Arase, "Computer simulation of skin color based on a multilayered skin model", *Skin Res. Technol.* **3**, 36 (1997).
8. P. Kubelka, "New Contributions to the Optics of Intensely Light-Scattering Materials". Part I, *J. Opt. Soc. Amer.* **38**(5), 448 (1948).
9. P. Kubelka, "New Contributions to the Optics of Intensely Light-Scattering Materials. Part II: Nonhomogeneous Layers", *J. Opt. Soc. Amer.* **44**(4), 330 (1954).
10. R. R. Anderson, J. Hu and J. A. Parrish, "Optical radiation transfer in the human skin and applications in in vivo remittance spectroscopy", *Proc. Symposium on Bioengineering and the Skin*, (1979) p. 253.
11. R. R. Anderson and J. A. Parrish, "The Optics of Human Skin", *J. Investigative Dermatology*, **77**(1), 13 (1981).
12. M. J. C. V. Gemert, S. L. Jacques, H. J. C. M. Sterenborg, and W. M. Star, "Skin Optics", *IEEE Trans. BME*, **36**(12), 1146 (1989).
13. S. D. Cotton and E. Claridge, "Developing a predictive model of human skin colouring", *Proc. SPIE*, **2708**, 814 (1996).
14. S. Yazawa, "Jintai shobui ni okeru hifu soshiki no hikaku kenkyu", *Igaku Kenkyu*, **7**, 1805 (1933). (*in Japanese*)
15. B. T. Phong, "Illumination for computer-generated pictures", *Comm. ACM* **18**(6), 311 (1975).
16. K. E. Torrance and E. M. Sparrow, "Theory for off-specular reflection from roughened surfaces", *J. Opt. Soc. Amer.* **57**, 1105 (1967).
17. R. Cook and K. Torrance, "A reflection model for computer graphics", *ACM Computer Graphics (SIGGRAPH 81)*, **15**(3), 307 (1981)
18. N. Tanaka, S. Tominaga, and T. Kawai, "Estimation of the Torrance-Sparrow reflection model from single multi-band image", *Proc. 15th Int. Conf. on Pattern Recognition*, **3**, 600 (2000)
19. S. Tominaga and N. Tanaka, "Refractive index estimation and color image rendering", *Pattern Recognition Lett.* **24**, 1703 (2003).
20. G. Wyszecki and W. S. Stiles, *Color Science: Concepts and Methods Quantitative Data and Formulae*, (Wiley, New York, 1982). pp-pp.
21. M. Doi, S. Ueda and S. Tominaga, "Frequency Analysis and Synthesis of Skin Color Textures" *IS&T/SID 10th Color Imaging Conference*, (IS&T, Springfield, VA, 2002) p. 233.
22. M. Doi, N. Tanaka and S. Tominaga, "Spectral Reflectance-Based Modeling of Human Skin and its Application", *Proc. 2nd European Conference on Color in Graphics, Imaging and Vision*, (IS&T, Springfield, VA, 2004), p. 388.